BIG SENTINEL DATA PROCESSING FOR MONITORING GROUND DEFORMATIONS

ASIAN CONFERENCE ON REMOTE SENSING ACRS 2019

Ioannis Papoutsis (1), Charalampos Kontoes (1), Alexis Apostolakis (1)

[1] Institute for Astronomy & Astrophysics, Space Applications and Remote Sensing, National Observatory of Athens, Metaxa & Vas. Pavlou, GR-15236 Athens, Greece

Email: ipapoutsis@noa.gr; kontoes@noa.gr; alex.apostolakis@noa.gr

KEY WORDS: Satellite Interferometry; Persistent Scatterer Interferometry; Ground Deformation; Sentinel-1; Rapid Damage Assessment, Data Cube

ABSTRACT: BEYOND is a Center of Excellence within the National Observatory of Athens which offers Earth Observation based services for monitoring natural disasters. BEYOND has a dedicated services pillar for monitoring geohazards from space. The cornerstone of the activity is geObservatory, an operational application for the timely mapping of ground deformation. geObservatory is activated in major geohazard events, such as earthquakes, volcanic activity, landslides, etc. and automatically produces a series of co-event differential interferograms based on Sentinel-1 Synthetic Aperture Radar data, to map the surface deformation associated with the event. The role of geObservatory is twofold: firstly, it provides to emergency management authorities with a rapid assessment of ground deformation, secondly it produces and maintains a global observatory of differential interferograms associated with catastrophic geo-events.

geObservatory has been tested throughout several activations in the past year and produced results on more than 25 occasions. The fully automatic application has proved very robust in swiftly producing ground deformation interferograms using big Sentinel data, towards a rapid first assessment of the damages. In this work we present the ground deformation results as produced by geObservatory and discuss the implications for assessing geohazard for three different events: the recent July 6th 2019 Southern California, USA, M7.1 earthquake, the August 19th 2018 M6.9 Lombok earthquake in Indonesia, and the volcanic activity in the Island of Hawaii that stared in May 2018.

1. INTRODUCTION

The new generation of Earth Observation satellites from the Sentinel missions generate huge amounts of data that are not easily integrated into processing chains outside the ground segments of space agencies. Very often, public and private institutions aiming at delivering end-user services based on Earth Observation data do not possess the computing power and storage capacity to profit from these new data flows.

The Helix Nebula Initiative started as a Public-Private-Partnership (PPP) with the goal of evaluating the needs of European compute -intense scientific research organisations and their exploitation of a Cloud Computing Infrastructure. The aim was to define a federated Cloud Computing Infrastructure that would provide resources and agreements needed for the IT-related operations from research institutions, enterprises (incl. SMEs), governments and society at large. Through the Helix Nebula Science Cloud initiative, a partnership was established between leading IT providers and some of Europe's biggest research centres that deployed and tested the infrastructure. One of the critical Use Cases of the Helix Nebula initiative is the one led by the European Space Agency (ESA), forming the ESA SuperSites Exploitation Platform (SSEP) Flagship.

The SSEP flagship use case enabled Helix Nebula to mature its federated Cloud architecture, and ultimately allowed ESA to analyse the feasibility and benefits of cloud deployments and broke new ground that ultimately lead the way to the development of the Thematic Exploitation Platform (TEP) initiatives.

In particular the Geohazard TEP (GEP) has provided a framework to ease the discovery (i.e. search) and retrieval (i.e. access) of EO data (remote-sensing and in situ). GEP is an exploitation platform for radar imagery in the context of geo-hazards, for the sharing of SAR data and the exploitation of interferometry processing on those data focusing on earthquake and volcano research. Currently there are several software tools for interferometric processing on the GEP.

However an end-to-end, fully automatic, robust, processing chain to rapidly generate interferograms following a major geohazard event is currently missing. According to our knowledge, there are only two currently initiatives to automatise interferometric processing, both in the USA and both of them relying on InSAR Scientific Computing Environment (ISCE) software. The first one is NASA funded SARVIEWS Hazard Monitoring1 from University of Alaska. It is implemented in the Amazon Cloud and produces interferometric SAR data over areas affected by natural disasters. The second one is NASA's Advanced Rapid Imaging and Analysis (ARIA2), a joint effort of California Institute of Technology (Caltech) and the Jet Propulsion Laboratory (JPL). ARIA is an infrastructure to generate interferometric imaging products in near real-time that can improve situational awareness for disaster response (Tung et al., 2019).

The motivation behind this work is twofold: firstly, to provides to emergency management authorities with a rapid assessment of ground deformation, secondly to produce and maintain a global observatory of differential interferograms associated with catastrophic geo-events, which can potentially populate a tailored Data Cube to allow further processing and analytics. Hence, the clear requirements to achieve this are the timely availability of appropriate interferometric

1 http://sarviews-hazards.alaska.edu

2 https://aria.jpl.nasa.gov/

pairs, a powerful infrastructure to quickly process the data and finally a fully automatic approach with minimum operator intervention as possible.

geObservatory by BEYOND Center of Excellence of the National Observatory of addresses these requirements. It is an operational application for the timely mapping of ground deformation. geObservatory (http://beyond-eocenter.eu/geohub), is activated in major geohazard events, such as earthquakes, volcanic activity, landslides, etc. and automatically produces a series of co-event differential interferograms (DInSAR) based on Sentinel-1 Synthetic Aperture Radar data, to map the surface deformation associated with the event.

2. DATA ACCESS

Access to Sentinel-1A&B Single Look Complex data that will feed an interferometric processing chain is fragmented. Currently, there are several Copernicus Hubs the provide access to Sentinel data. These include the core Copernicus Hubs, such as Open Access Hub (formerly SciHub), the four Data and Information Access Services (DIAS) Hubs, the ApiHub and the Cop Hub. In addition, the European Space Agency (ESA) in order to allow complementary access to Sentinel data and/or to specific data products or distribution channels, has established the National Collaborative Ground Segments initiative. There are 23 National Collaborative Ground Segments, indicatively the HNSDMS (Greece, https://sentinels.space.noa.gr/), the CODE-DE (Germany, https://code-de.org/), the FinHub (Finland, http://nsdc.fmi.fi/services/service_finhub_overview) and PEPS (France, https://peps.cnes.fr/rocket/).

The main issue of this fragmented data access is that the hubs available have different data offers. This affects parameters, such as the availability of different missions and different products per sensor, the geographic coverage, the maximum concurrent downloads allowed, the data rolling policy, i.e. the time span of the data archive, etc. In addition to the data offer variability, the hubs experience different performances in terms of several Key Performance Indicators (KPIs), including, the download speed, the query response times, the operational availability, the product latency, i.e. the difference the between sensing time and the time it is available to download in a specific hub. In practice even for the same hub there is intra-day, and intra-product variability in terms of KPIs.

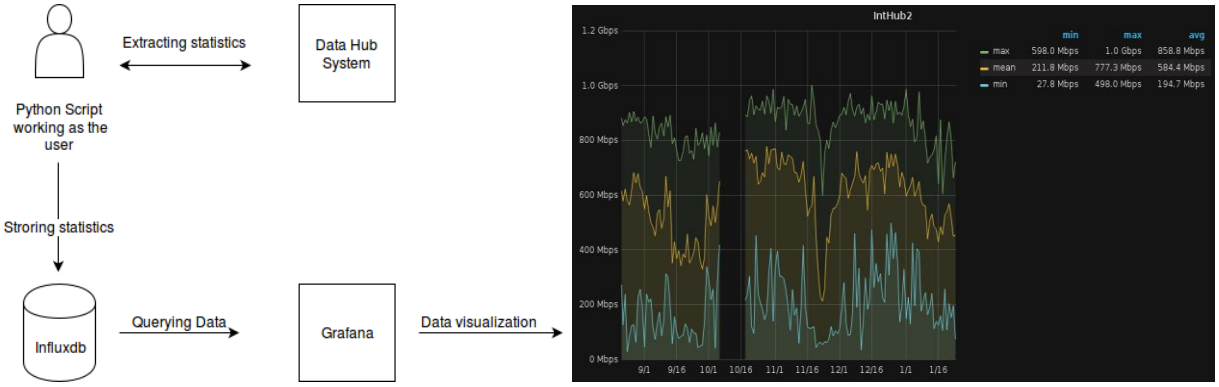

Figure 1. Architecture for the benchmarking exercise

Figure 2 and Figure 3 show the results of a benchmarking exercise we performed to evaluate the performance of the different Copernicus Hubs. The measurements were extracted with scripts written in Python that represent a user in the cloud using the GEANT network (Figure 1). The user polled the Hubs in a continuous fashion, on a daily basis and in specific schedules for each measurement. The measurements were collected using an InfluxDB database. Alongside InfluxDB we also used a Grafana3 instance to visualize the measured data dynamically.

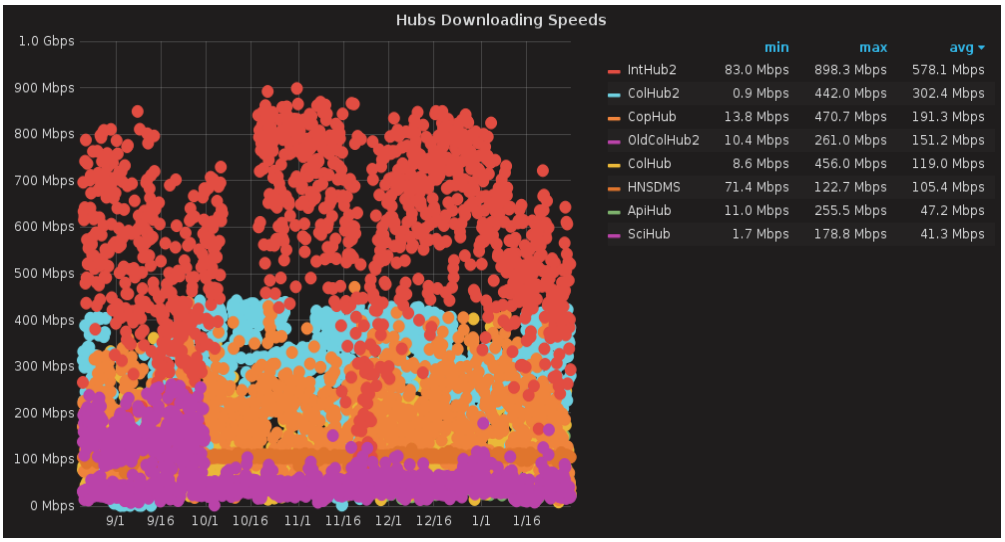

Figure 2. Variability in the download speed of the different Copernicus Sentinels Hubs

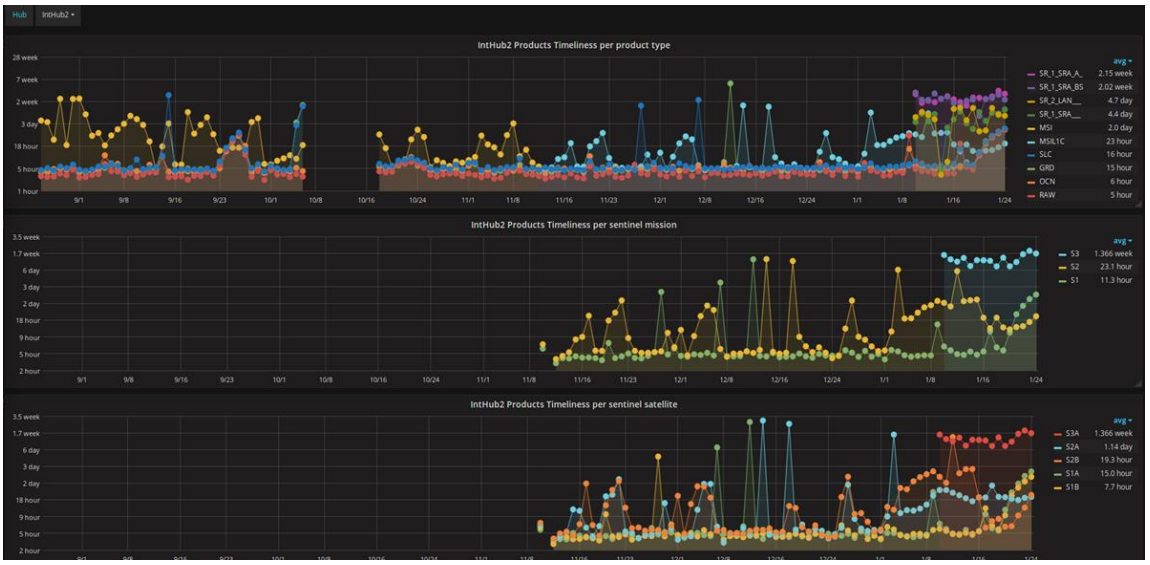

Figure 3. Product latency variability for a single hub, in this case the Copernicus International Hub.

Our idea to cope with this Hub performance variability and to ensure the rapid mapping of the deformation following a catastrophic geo-event, we developed an umbrella application to federate access to Sentinel data. The architecture of the application is shown in Figure 4, while the system was developed in the framework of the European Commission Horizon 2020 project

3 https://grafana.com/

There are two synchronization steps for the application. Data synchronization takes place considering the data offer of the Hellenic Mirror Site5. In this step, actual data are moved and stored within the umbrella application. The second step is metadata synchronization, where a metadata catalogue is populated and regularly updated by registering the products that are available on other Hubs, such as the Core Copernicus Hubs, the DIAS Hubs and some selected National Collaborative GS. A user requesting a list of Sentinel products will be served transparently by our application, and the products will be downloaded by several hubs, depending on product availability. If the same product exists in more than one hub, then performance criteria are applied (e.g. response time and real-time bandwidth of the link) to select the best performing hub. The front-end of the application is based on the Data Hub Software (DHuS) by ESA and incorporates OpenData and OpenSearch APIs.

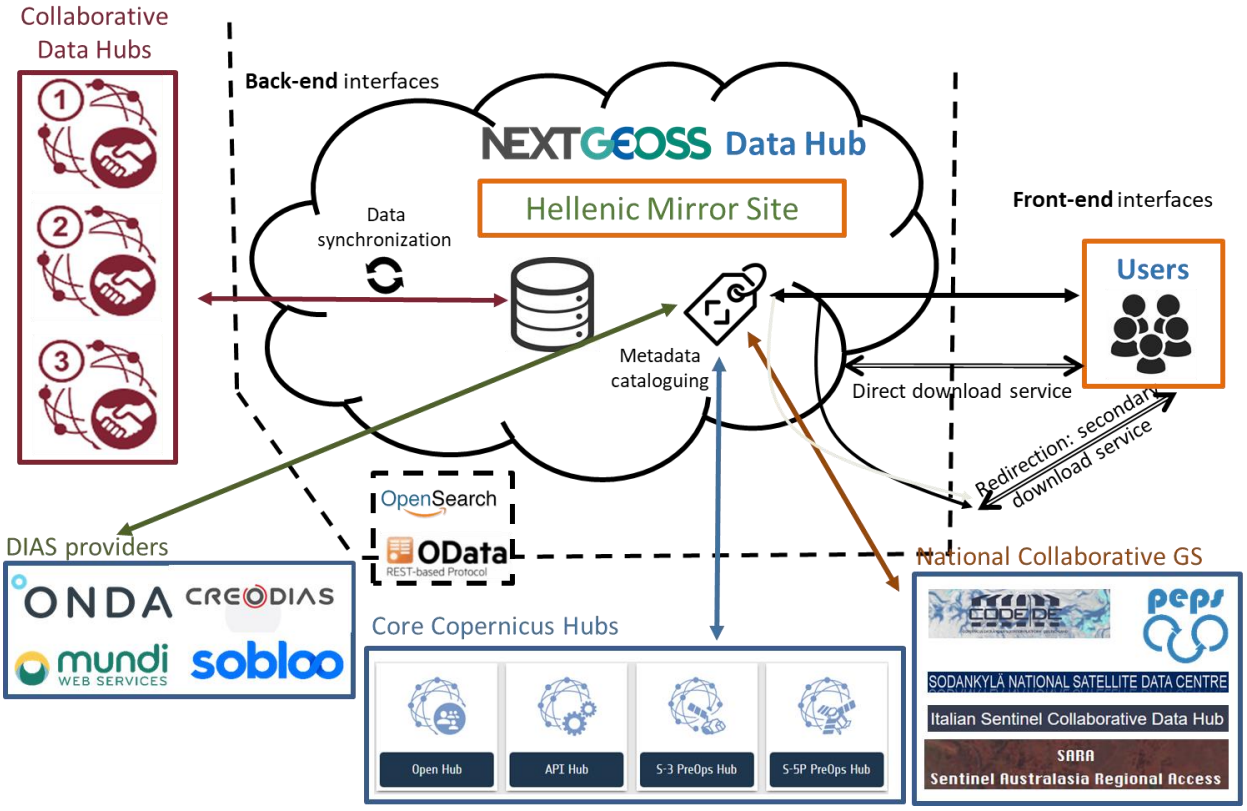

Figure 4. Application architecture for the federation of Sentinel data

The main advantage of linking federated Copernicus Sentinels Hubs is the enhanced timeliness and reduced lead times for accessing Sentinel products, which is especially important for disaster management applications such as geObservatory. Furthermore, our solution provides access to a single hub instead of looking across several Sentinel Hubs to find the appropriate products, while it provides access to all Sentinel mission data with no geographic restrictions. Finally, by exploiting Hub diversity there is less performance variability, and this makes a fully

4 https://nextgeoss.eu/

5 https://sentinels.space.noa.gr/

automatic processing chain that relies on the availability of its inputs more robust.

3. geObservatory BACK-END

geObservatory is activated in major geohazard events (earthquakes, volcanic activity, landslides,etc.) and automatically produces a series of Sentinel-1 based co-event differential interferograms (DInSAR) to map the surface deformation associated with the event.

The application is activated in two ways. Either manually - an authorized user provides to the application a json file delineating the Area of Interest and registering the timestamp of the event - or automatically. In the automatic activation geObservatory connects to the European-Mediterranean Seismological Centre (EMSC) and is triggered when a major earthquake occurs. Criteria for the activation of geObservatory is the magnitude of the earthquake and its focal depth.

After the system is activated, the application automatically scans different Copernicus hubs, including the Greek Collaborative Ground Segment, to find the appropriate Sentinel-1 satellite data for interferometry. The scanning is performed using the umbrella application of Figure 4. When an appropriate interferometric pair is identified, considering restrictions in sensing time, sensing mode (descending or ascending), and geometry (orbit number), a fully automatic differential interferometry processing chain is triggered Figure 5. The processing modules are found within the commercial software SARscape (Peternier et al., 2013).

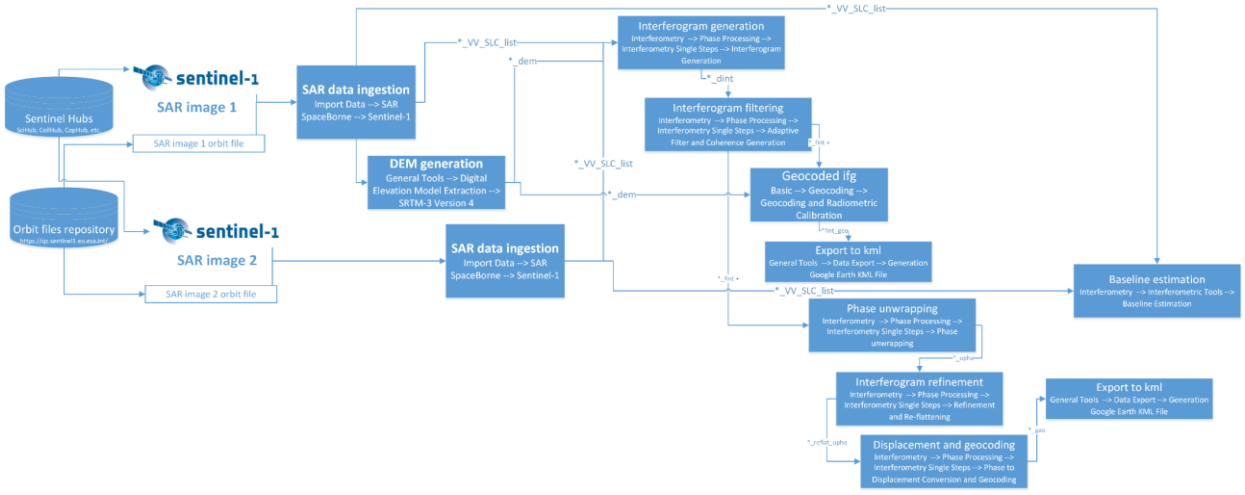

Figure 5. Interferometric processing chain triggered by geObservatory

For each activation, geObservatory produces several pre-seismic and all available co-seismic interferograms. Since the application has global coverage, it may happen that geObservatory serves more than one activation at each instance. Therefore there is a need to swiftly orchestrate priorities and execution steps. This is the task of the Application Orchestrator Server (Figure 6). The Products collection and Task scheduling Service is written in python. This program initiates the request processing, finds and downloads the necessary satellite inputs and controls the output production tasks. The Service Metadata Database (postgresql) contains processing information, input and output metadata. The ENVI SARscape module is the interferogram production engine. The Products collection and Task scheduling Service executes commands from ENVI SARscape module using IDL scripts in order to create the interferograms.

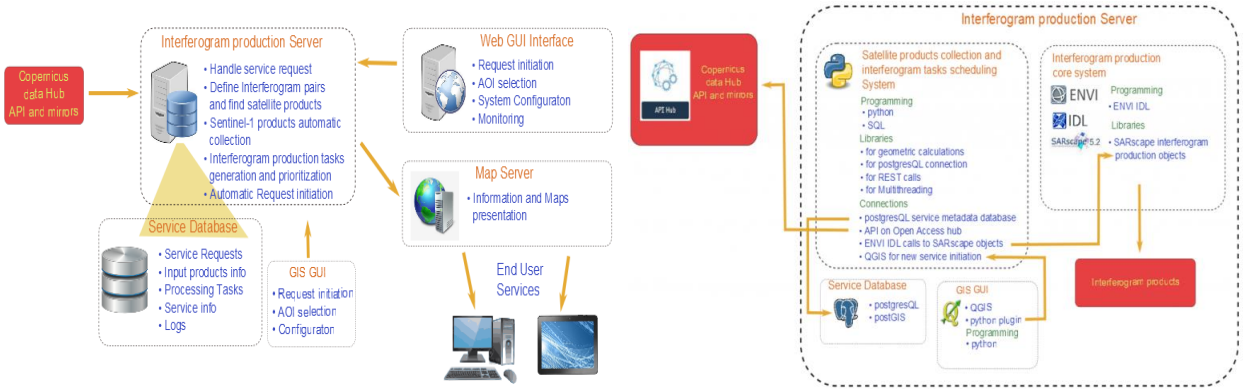

Figure 6. geObservatory orchestrator back-end components

The interferograms created are then available for visualization and download through a dedicated front-end. It provides quick-look interferograms in PNG format, a high resolution tiff available for download and an online viewer that uses Leaflet JavaScript technology to project and display the interferograms.

4. geObservatory ACTIVATIONS

geObservatory has been tested throughout several activations in 2018 and 2019 and produced results on more than 45 occasions. The fully automatic application has proved very robust in producing ground deformation interferograms using big Sentinel data, towards a rapid first assessment of the damages. In this work we present the ground deformation results as produced by geObservatory for three different events: the recent July 6th 2019 Southern California, USA, M7.1 earthquake, the August 19th 2018 M6.9 Lombok earthquake in Indonesia, and the volcanic activity in the Island of Hawaii that started in May 2018. This is an indicative list of events to showcase the ability of the system to cope with events with different characteristics. We do not dive in detail in the geophysical implications and interpretations of the observed deformation patterns.

1. 2019 earthquake in Southern California, USA

The 2019 Ridgecrest earthquakes of July 4 (Mw 6.6) and 5 (M_w 7.1) occurred north and northeast of the town of Ridgecrest, California (approximately 200 km north-northeast of Los Angeles). The USGS issued a red alert for economic losses meaning that extensive damage is probable, and the disaster is likely widespread. Estimated economic losses were at least $1 billion dollars, less than 1 % of GDP of the United States.

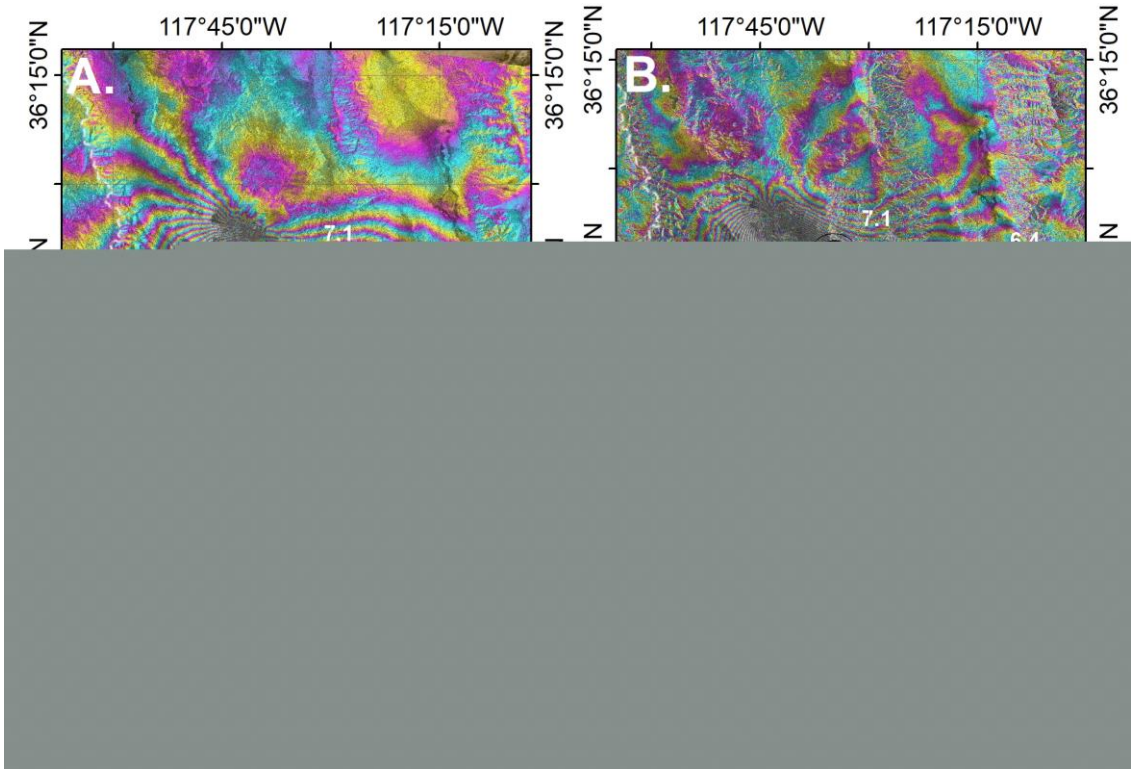

Figure 7. Wrapped interferograms for the (A.) descending and (B.) ascending track, capturing line-of-sight ground deformation for the Mw 6.6 and Mw 7.1, of the 4th and 5th of July 2019 respectively Southern California earthquake.

geObservatory was activated for the event of the 5th of July 2019. The first available image arrived on the 10th of July 2019, in ascending mode. The ascending interferogram was produced on the 16th of July, a few hours after the reception of the SAR image. Figure 7 highlights the strong line-of-sight ground deformation pattern associated with this earthquake. To our knowledge no work has been published yet that considers the ground deformation as measured from Synthetic Aperture Radar.

2. 2018 earthquake in Lombok, Indonesia

In 19 August 2018 a major earthquake struck with high intensity on the northeast corner of Lombok and northwest Sumbawa at 22:56 local time, a few km to the east of the series of quakes that had been rocking the area for the past 3 weeks. The earthquake occurred on the Flores Back Arc Thrust Belt, probably on a different thrust fault. There were 14 deaths as an aftermath of the event.

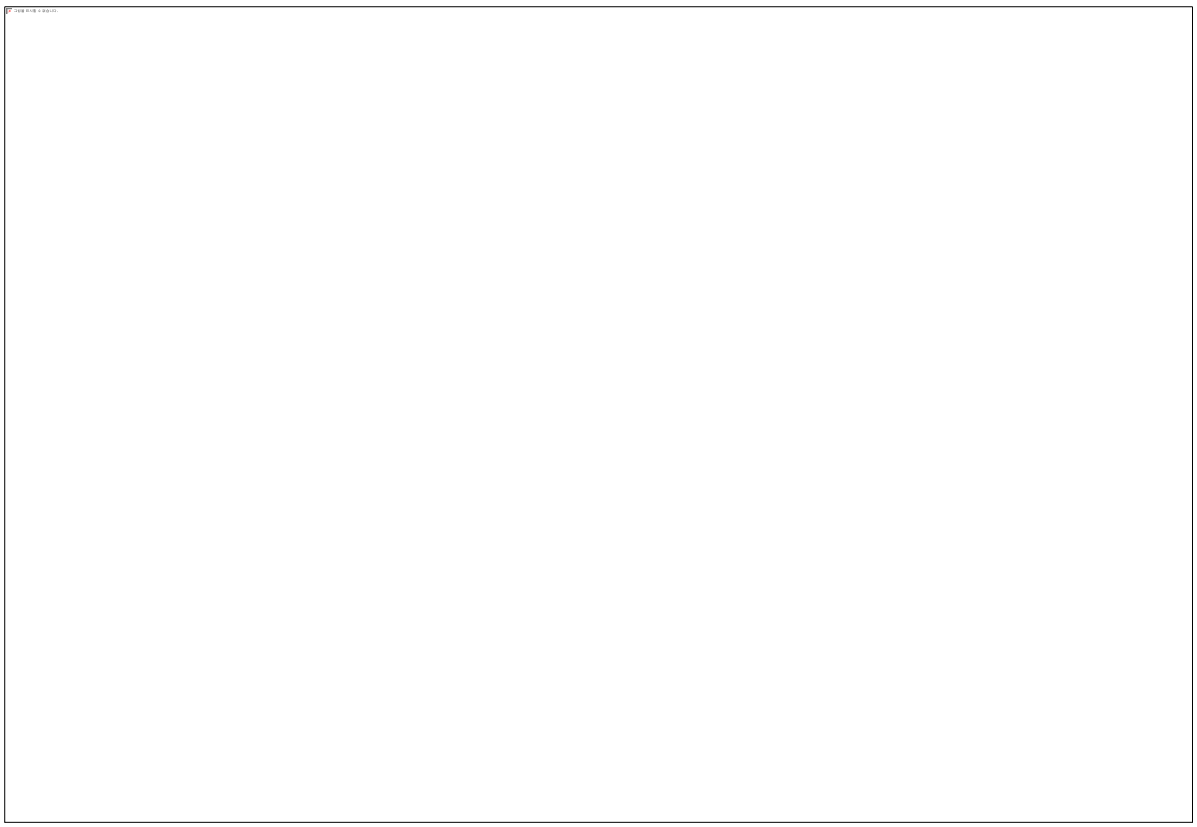

Figure 8. Wrapped interferograms for the (A.) descending and (B.) ascending track, capturing line-of-sight ground deformation for the Mw 6.9, of the 19th of August 2018 Lombok (Indonesia) earthquake.

Agustan et al., 2019 used Sentinel-1 based interferometry to estimate the deformation of the series of earthquakes that hit Lombok Island in July and August 2018 with magnitude 6 class. Ferrario, 2019, analyzed the landslides triggered by the 2018 Lombok seismic sequence, using high-resolution satellite imagery to map 9319 landslides after the 19/08/2018 event. geObservatory promptly produced a series of pre-seismic and co-seismic interferograms, which are presented in Figure 8.

3. 2018 volcanic activity in Hawaii, USA

During 26/4-2/5/2018, intense micro-seismic activity occurred in the wider area of the Kīlauea volcano in Hawaii. On Thursday 3/5/2018 a volcanic crack appeared near the road network in lower Puna region, from which lava and hot steam appeared. The Civil Protection instructed residents of the Puna community (~10,000) to leave their homes immediately. On Friday, May 4, 2018, a powerful 6.5 earthquake hit Puna (Figure 9), the largest in the past 43 years. By May 27, 2018, 24 fissures had erupted lava in or near the Leilani Estates and Lanipuna Gardens subdivisions.

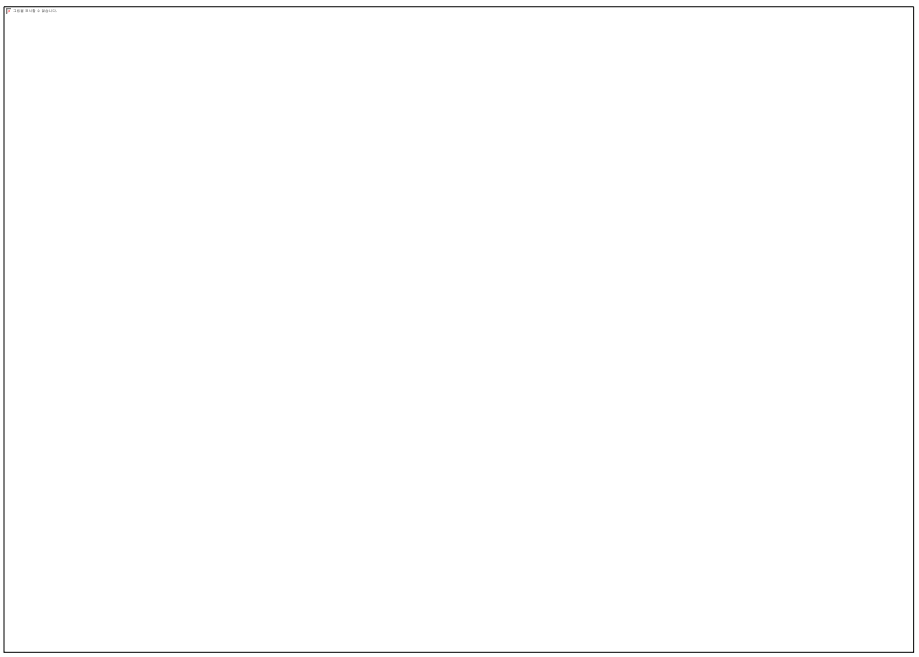

Figure 9. Seismicity in Kilauea volcano, Hawaii (source: USGS)

By August 7, 35 km^2 of land had been covered by lava flows. The eruption had almost completely subsided, and on December 5, it was declared to have ended after three months of inactivity. Recovery efforts were estimated to cost more than $800 million.

Radar interferometry was used extensively to understand and interpret the phenomenon. Lundgren et al., 2019, studied the topographic changes due to the volcanic eruption. Chen et al., 2019 focused on the triggering of the earthquake due to magma dike intrusion. Babu and Kumar, 2019, performed interferometric time series analysis using Small BAseline Subset techniques to detect subsidence at the Kilauea summit. Neal et al., 2019 present a summary of the eruption sequence along with a variety of geophysical observations collected by the Hawaiian Volcano Observatory. Finally, Wang et al., 2019 used extensive interferometric measurements to estimate the triggered slip of active normal faults of Kīlauea volcano's south flank.

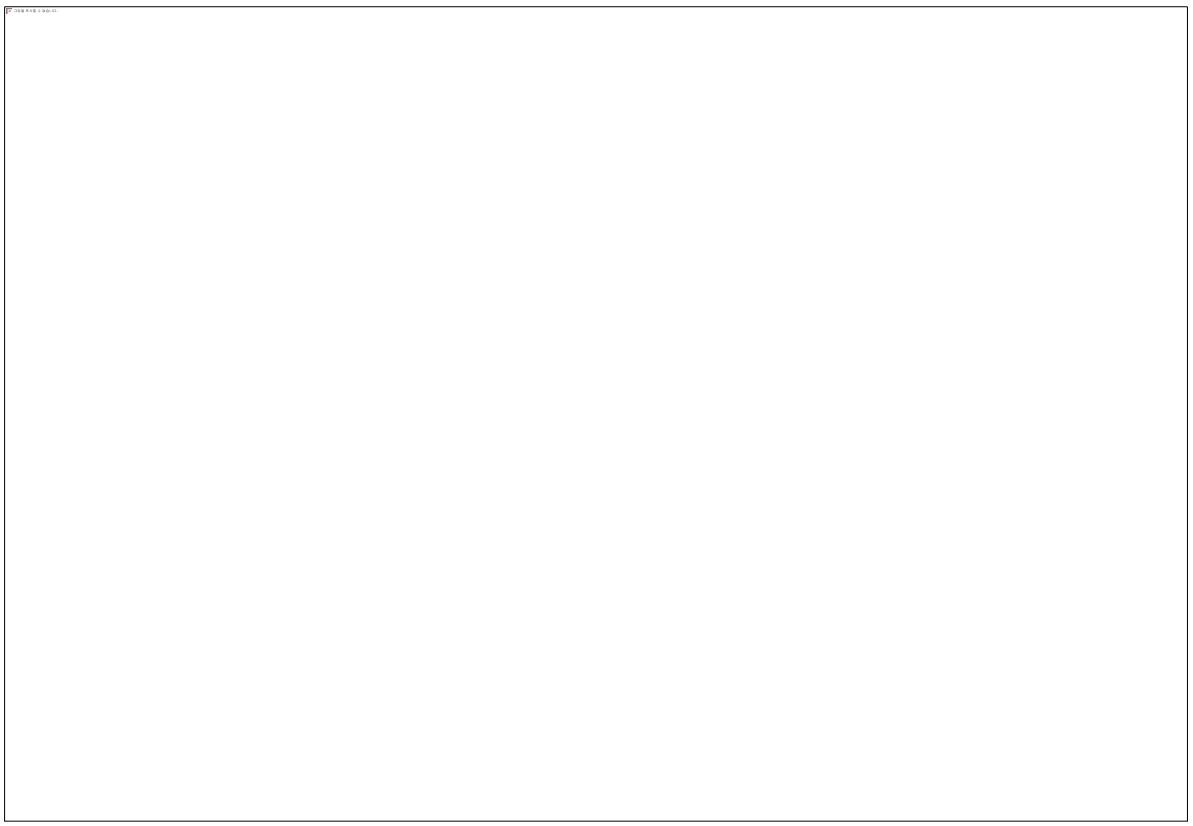

Figure 10. Wrapped interferograms for the (A.) descending and (B.) ascending track, capturing line-of-sight ground deformation in Kilauea volcano, Hawaii. A. includes deformation fringes due to the M6.5 earthquake, while B. contains deformation due to volcanic activity only.

geObservatory was activated to monitor both the volcanic activity and the impact of the earthquake Figure 10. Given the tectonic setting of the region (Figure 11), intense subsidence was observed at the top of the volcano as magma material moved along the East Rift Zone and escaped to the eastern edge of the fault. The maximum deformation along this zone, located between the top of the volcano and the area where the lava was firstly observed, is approximately 60-70 cm.

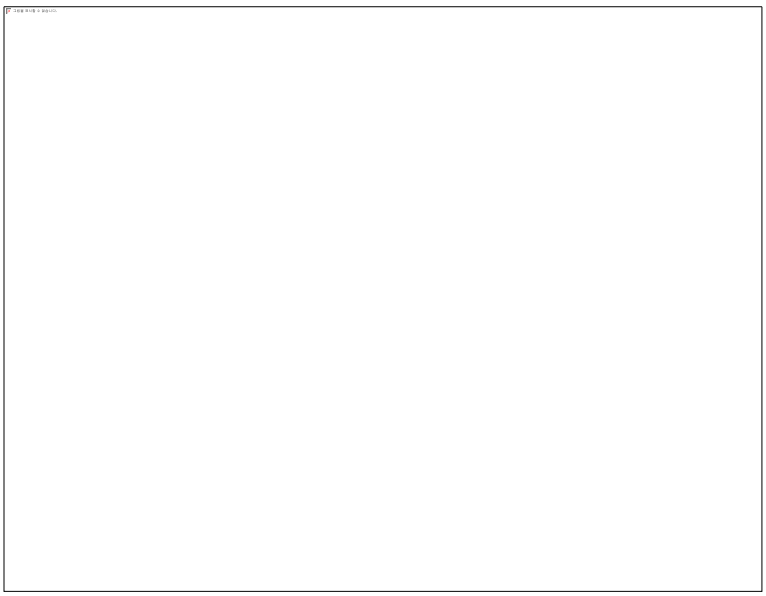

Figure 11. Tectonic setting in Kilauea volcano region (source: USGS)

5. CONCLUSIONS

geObservatory is an end-to-end fully automatic application that rapidly provides information on the ground deformation associated with major geohazard events. It employs a new SAR data retrieval module that is linked with several Copernicus Sentinel Hubs to ensure robustness and timeliness of the service. A typical interferometric processing chain is executed on a powerful server to produce pre-seismic and co-seismic differential interferograms, while the interferometric products are made available for viewing and downloading in a front-end web environment.

In one year of pilot operation, geObservatory has been very fast in producing interferograms, a few hours after the first post-seismic SAR image becomes available in any of the available hubs. In addition, due to the several activations of the application, we have produced and made publicly available a unique geodatabase of interferograms covering major geo-events. These interferograms can be reused by the scientific community to enhance our knowledge on tectonic, earthquake and volcano research.

ACKNOWLEDGEMENTS

Authors acknowledge the Hellenic National Sentinel Data Mirror Site (**https://sentinels.space.noa.gr/**) for providing free access to Sentinel-1 and Sentinel-2 images. This work has been partly funded by NextGEOSS European Commission H2020 project.

REFERENCES

Agustan, Rahma N. Hanifa, Yudi Anantasena, M. Sadly and Takeo Ito, Ground Deformation Identification related to 2018 Lombok Earthquake Series based on Sentinel-1 Data, IOP Conference Series: Earth and Environmental Science, 280, 2019.

Babu Arun, Shashi Kumar, SBAS interferometric analysis for volcanic eruption of Hawaii island, Journal of Volcanology and Geothermal Research, Volume 370, 2019, 31-50.

Casu, F.; Elefante, S.; Imperatore, P.; Zinno, I.; Manunta, M.; De Luca, C.; Lanari, R. SBAS-DInSAR parallel processing for deformation time-series computation. IEEE J. Sel. Top. Appl. Earth Obs. Remote Sens. 2014, 7, 3285–3296

Chen, K., Smith, J. D., Avouac, J.-P., Liu, Z., Song, Y. T., & Gualandi, A. (2019). Triggering of the Mw 7.2 Hawaii earthquake of 4 May 2018 by a dike intrusion. Geophysical Research Letters, 46, 2503– 2510.

De Luca, C.; Cuccu, R.; Elefante, S.; Zinno, I.; Manunta, M.; Casola, V.; Rivolta, G.; Lanari, R.; Casu, F. An On-Demand Web Tool for the Unsupervised Retrieval of Earth's Surface Deformation from SAR Data: The P-SBAS Service within the ESA G-POD Environment. Remote Sens. 2015, 7, 15630-15650.

Manunta Michele; Claudio De Luca ; Ivana Zinno ; Francesco Casu ; Mariarosaria Manzo ; Manuela Bonano ; Adele Fusco ; Antonio Pepe ; Giovanni Onorato ; Paolo Berardino; Prospero De Martino ; Riccardo Lanari 2019. The Parallel SBAS Approach for Sentinel-1 Interferometric Wide Swath Deformation Time-Series Generation: Algorithm Description and Products Quality Assessment, IEEE Transactions on Geoscience and Remote Sensing, 57(9), pp 6269-6281.

Fattahi H., P. Agram, and M. Simons, "A network-based enhanced spectral diversity approach for TOPS time-series analysis," IEEE Trans. Geosci. Remote Sens., vol. 55, no. 2, pp. 777–786, Feb. 2017.

Ferrario, M.F. Landslides triggered by multiple earthquakes: insights from the 2018 Lombok (Indonesia) events, Nat Hazards (2019) 98: 575.

Lundgren, P. R., Bagnardi, M., & Dietterich, H. (2019). Topographic changes during the 2018 Kīlauea eruption from single-pass airborne InSAR. Geophysical Research Letters, 46, 9554– 9562.

Neal A., The Kīlauea Volcano erupted 0.8 cubic kilometers of magma, which triggered a summit collapse over the 3 months of the eruption. Science, 2019, 367-374

Peternier A., M. Defilippi, P. Pasquali, A. Cantone, R. Krause, R. Vitulli, F. Ogushi, A. Meroni, Performance analysis of GPU-based SAR and interferometric SAR image processing, Asia-Pacific Conference on Synthetic Aperture Radar (APSAR), Tsukuba, 2013.

Tung S., E. J. Fielding, D. P. S. Bekaert, T. Masterlark, Rapid geodetic analysis of subduction zone earthquakes leveraging a 3D elastic Green's function library. 2018, Geophys. Res. Lett., 44

Wang, K., MacArthur, H. S., Johanson, I., Montgomery-Brown, E. K., Poland, M. P., Cannon, E. C., et al. (2019). Interseismic quiescence and triggered slip of active normal faults of Kīlauea Volcano's south flank during 2001–2018. Journal of Geophysical Research: Solid Earth, 124.

Zinno I. et al., "A first assessment of the P-SBAS DInSAR algorithm performances within a cloud

computing environment," IEEE J. Sel. Topics Appl. Earth Observ. Remote Sens., vol. 8, no. 10, pp. 4675–4686, Oct. 2015.

Zinno I. et al., "Cloud computing for Earth surface deformation analysis via spaceborne radar imaging: A case study," IEEE Trans. Cloud Comput., vol. 4, no. 1, pp. 104–118, Jan. 2016.

Zinno I., F. Casu, C. D. Luca, S. Elefante, R. Lanari, and M. Manunta, "A cloud computing solution for the efficient implementation of the P-SBAS DInSAR approach," IEEE J. Sel. Topics Appl. Earth Observ. Remote Sens., vol. 10, no. 3, pp. 802–817, Mar. 2017.